THE JOURNAL OF PHYSICAL CHEMISTRY Letters

Letter

Cite This: J. Phys. Chem. Lett. 2018, 9, 2979−2984

pubs.acs.org/JPCL

Structural Motifs in Cold Ternary Ion Complexes of Hydroxyl-Functionalized Ionic Liquids: Isolating the Role of Cation−Cation Interactions

Fabian S. Menges,[†] Helen J. Zeng,[†] Patrick J. Kelleher,[†] Olga Gorlova,[†] Mark A. Johnson,*[,†] Thomas Niemann,[‡,§] Anne Strate,[‡,§] and Ralf Ludwig*[,‡,§]

[†]Sterling Chemistry Laboratory, Yale University, New Haven, Connecticut 06520, United States

[‡]Department of Chemistry, University of Rostock, 18059 Rostock, Germany

[§]Leibniz-Institut für Katalyse e.V., Albert-Einstein-Strasse 29a, 18059 Rostock, Germany

Supporting Information

ABSTRACT: We address the competition between intermolecular forces underlying the recent observation that ionic liquids (ILs) with a hydroxyl-functionalized cation can form domains with attractive interactions between the nominally repulsive positively charged constituents. Here we show that this behavior is present even in the isolated ternary $(HEMIm^+)_2NTf_2^-$ complex ($HEMIm^+$ = 1-(2-hydroxyethyl)-3-methylimidazolium) cooled to about 35 K in a photodissociation mass spectrometer. Of the three isomers isolated by double resonance techniques, one is identified to exhibit direct contact between the cations. This linkage involves a cooperative H-bond wherein the OH group on one cation binds to the OH group on the other, which then attaches to the basic N atom of the anion. Formation of this motif comes at the expense of the usually dominant interaction of the acidic $C_{(2)}H$ group on the Im ring with molecular anions, as evidenced by isomer-dependent shifts in the $C_{(2)}H$ vibrational fundamentals.

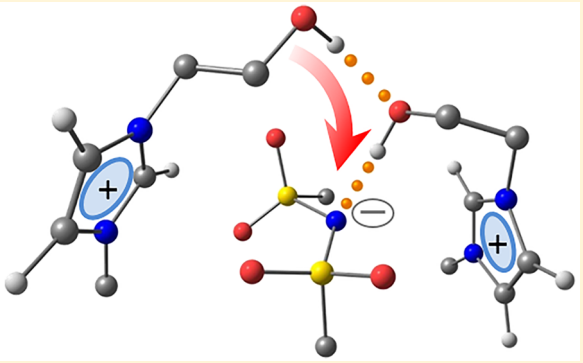

The development of room-temperature ionic liquids (RTILs) has accelerated in recent years as their properties become increasingly tailored[1,2] to facilitate chemical processes ranging from alternative, environmentally friendly solvents for chemical syntheses[3−5] to spacecraft propellants.[6−8] Because ILs are often heterogeneous at the molecular scale,[9−12] optimizing their properties for particular applications from first-principles has proven to be challenging,[8,13−22] and there are open fundamental questions about the intramolecular distortions and local contact motifs between the ionic constituents.[23−25] For example, recent bulk spectroscopic results (FT-IR) have been reported that indicate direct points of contact between cations, denoted (c−c) interactions,[26,27] that arise from cooperative hydrogen bonds involving the OH groups on hydroxyl-functionalized systems. In those cases, the spectroscopic signatures of hydrogen bonding in the OH stretching region were observed to become more prominent at lower (∼213 K) temperatures, but the diffuse nature of the bands allowed only a qualitative picture of the local interactions. Here we focus on the isolated cluster ion consisting of two cations and one anion, denoted hereafter as (2,1), which are the smallest systems capable of displaying an anion-mediated, attractive interaction between molecular cations. The issues at play are indicated in the schematic arrangements of the ternary ionic complex displayed in Scheme 1. The arrangement shown on the right in Scheme 1, with the anion sandwiched between the cations, has been observed in many (2,1) complexes that do not have OH groups.[28] The formation of a direct contact between the hydroxyl groups with short hydrocarbon tails (left structure in Scheme 1) requires a distortion of this quasi-symmetrical arrangement. For such a (c−c) interaction to occur, it would appear that the increased Coulomb repulsion between the positive charge centers and loss of one OH attachment to the anion would have to be somehow compensated by the H-bond linkage. Our goal in this work is therefore to identify a microscopic (2,1) system displaying this type of (c−c) motif in order to clarify the nature of the individual contacts that drive its stability.

We specifically focus on the two cationic imidazolium derivatives ($EMIm^+$ and $HEMIm^+$) depicted in Scheme 2, complexed to NTf_2^- (bis(trifluoromethylsulfonyl)imide), one of the most widely used anions in ILs.[1] These cations were chosen because recent studies[17,23,24,29−34] have reported a spectroscopic way to measure the strength of the interaction between the most acidic position ($C_{(2)}H$) on the positively charged imidazolium ring and various anions (halides, BF_4^-).

Received: April 11, 2018
Accepted: May 11, 2018
Published: May 11, 2018

DOI: 10.1021/acs.jpclett.8b01130
J. Phys. Chem. Lett. 2018, 9, 2979−2984

Scheme 1. Illustration of Competing Interactions at Play in an Ionic Liquid with a Hydroxyl-Functionalized Cation in the Positively Charged, Gas-Phase Ternary Complex

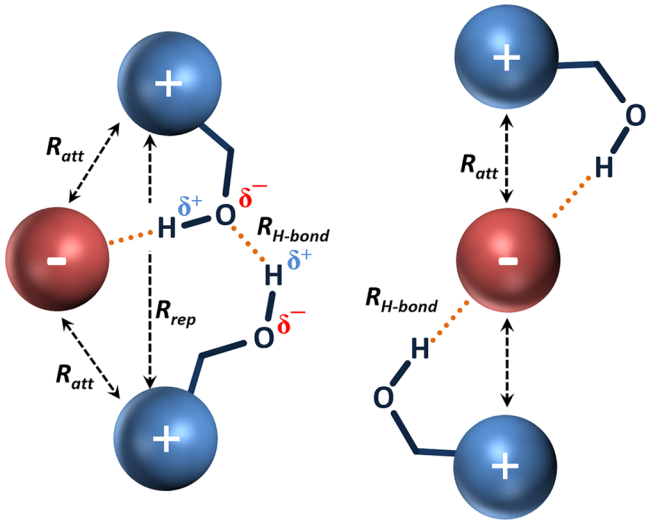

Scheme 2. Structures of 1-Ethyl-3-methylimidazolium ($EMIm^+$), 1-(2-Hydroxyethyl)-3-methylimidazolium ($HEMIm^+$), and Bis(trifluoromethylsulfonyl)imide (NTf_2^-) Ions

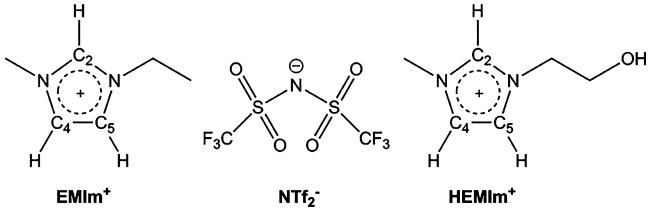

This is accomplished by isolating the behavior of the vibrational fundamental associated with the isotopologue that is selectively deuterated at the $C_{(2)}$ position ($C_{(2)}D$) on the ring.[28,31,32] When combined with the highly responsive nature of the OH stretching fundamental to its local environment, we demonstrate how the locations of the $C_{(2)}H(D)$ and OH(D) stretching transitions provide sensitive spectroscopic reporters for the intermolecular interactions at play in the ternary ion assemblies. Specifically, by comparing the spectral behavior of the $EMIm^+$ (2,1) complex with that of the hydroxylated derivative ($HEMIm^+$), we establish that an H-bond linkage between the cations occurs even in this remarkably small complex. This allows us to reveal the detailed competition between the OH and CH groups for H-bonding attachment sites on NTf_2^- that underlie an attractive (c-c) assembly motif.

We characterize the structures of the ternary complexes with two cations and one anion by analyzing their vibrational spectra, which are obtained at low temperature (~35 K) through the use of mass-selective, cryogenic ion trapping techniques.[35] This method acquires spectra in a linear action mode by infrared photodissociation of weakly bound N_2 adducts.[9,31,32,35−37] Furthermore, where appropriate, structural motifs of different isomeric structures adopted by these charged clusters are isolated through application of isomer-selective, two-color IR−IR double resonance spectroscopy.[38] The structural implications of the resulting band patterns are discussed in the context of calculated spectra for various structural candidates obtained at the B3LYP-D3/6-31+G(d) level of theory.[39−44]

Figure 1 presents the vibrational spectra measured for the $EMIm^+$ and $HEMIm^+$ ions (Figure 1a,c, respectively) along

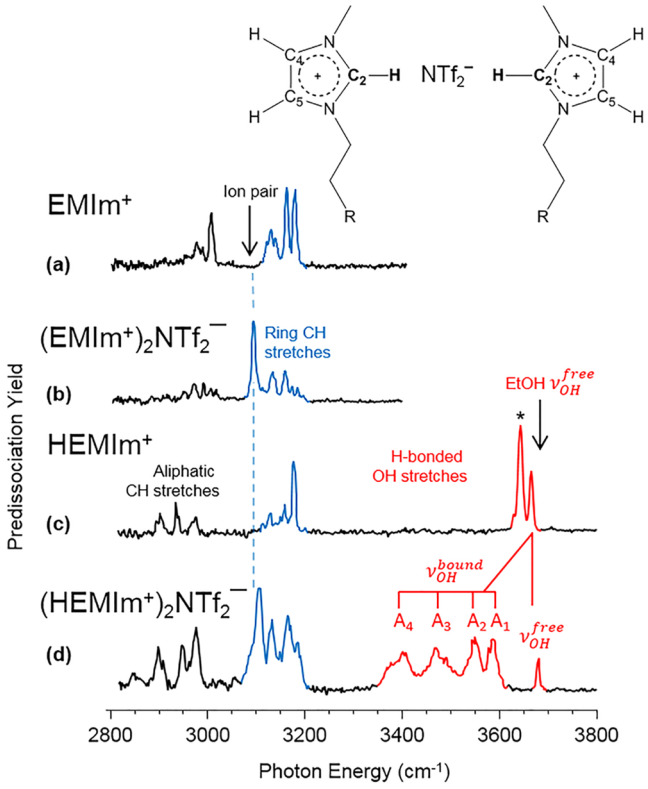

Figure 1. Photodissociation spectra of N_2-tagged (a) $EMIm^+$, (b) $(EMIm^+)_2NTf_2^-$, (c) $HEMIm^+$, and (d) $(HEMIm^+)_2NTf_2^-$. The OH stretches in traces (c) and (d) are colored red, with * in (c) representing an isomer where the N_2 tag is bound to the free OH (see Figure S1). The labels A_1, A_2, A_3, and A_4 denote H-bonded OH features in the ternary complex (d). In trace (b), the strongest band of the ring CH features (blue) lies close to the $C_{(2)}H$ feature reported earlier for the [EMIm][NTf_2] neutral ion pair[23,33,34] (arrow in trace (a)). The OH stretch fundamental of bare ethanol is indicated by an arrow at the right of trace (c).[58] R = OH for $HEMIm^+$ and H for $EMIm^+$. Measured transition energies are tabulated in Table S1.

with those of the corresponding (2,1) clusters with NTf_2^- (Figure 1b,d) in the spectral region associated with the key fundamentals involving the ring CH (blue) and OH (red) stretching modes. Energies of the key transitions are listed in Table S1. The CH multiplet near 3150 cm^{-1} has been traced to strong mixing among the three aromatic CH stretches (labeled C_2, C_4, and C_5 in Scheme 2) as well as to Fermi-type interactions involving overtones of the corresponding bending modes.[23,31−34,45] Nonetheless, both cations exhibit significant red shifts of these features upon complexation with the NTf_2^- anion, with the strongest member of the multiplet appearing lowest in energy. The fact that this feature occurs at essentially the same frequency in both ternary systems suggests that similar interactions are in play between the imidazolium ring and the anion. Moreover, we note that a similar band was observed in the [EMIm][NTf_2] neutral ion pair (arrow in Figure 1a),[23,33,34] indicating that this is characteristic of the preferred binding motif between the $EMIm^+$ ring and the NTf_2^- anion.

DOI: 10.1021/acs.jpclett.8b01130
J. Phys. Chem. Lett. 2018, 9, 2979−2984

The spectrum of the ternary $(HEMIm^+)_2NTf_2^-$ complex (Figure 1d) also includes an extended suite of transitions in the OH stretching region (labeled A_1, A_2, A_3, and A_4) that appear below the location of a free OH group (for example, in isolated ethanol, arrow in Figure 1c), with substructure evident on the lowest two (A_3 and A_4) features. We note that the asymmetric doublet in the $HEMIm^+$ spectrum near 3650 cm^{-1} arises from attachment of the N_2 tag (* in Figure 1c) to the free OH group, as discussed further in the SI (Figure S1). The red-shifted bands (A_1–A_4) in the (2,1) spectrum occur in the region corresponding to fundamentals of OH groups that strongly interact with anionic domains.[38,46−51] The picture that emerges from qualitative behavior of the ring CH and OH stretching bands is therefore that at least one of these two groups (available from the two cations) is strongly interacting with the anion. Moreover, the plethora of transitions in the OH stretching region raises the specter that different isomers may contribute to the pattern (as opposed to reflecting strong anharmonic coupling, which is also known to result in soft mode progressions built on OH stretching fundamentals[52]).

Recognizing that the $HEMIm^+$ ion presents two primary contact points, the $C_{(2)}H$ and OH groups (Scheme 2), for interaction with the anion, the key issue regards whether these docking motifs compete for attachment sites on the anion. To establish the activity of the $C_{(2)}H$ groups, we obtained the spectra of the $HEMIm^+$ isotopologue with deuterium atom substitutions at both the $C_{(2)}$ and OH positions (denoted $d_{(2)}$-$DEMIm^+$, Figure 2a), its ternary complex with NTf_2^- (Figure 2c), and, for comparison, that of the analogous ternary complex with the $d_{(2)}$-$EMIm^+$ ion (Figure 2b). As mentioned above, the spectral response of the $C_{(2)}D$ group is free of the anharmonic interactions that complicate the interpretation of the coupled oscillators in the CH stretching region. As expected, the $C_{(2)}D$ fundamental appears as an isolated band in the bare ion spectrum, ($\nu^{free}_{C_{(2)}D}$ in Figure 2a). Interestingly, the OD pattern in the $(d_{(2)}\text{-}DEMIm^+)_2NTf_2^-$ spectrum (Figure 2c) is very similar to that of the OH pattern observed in the $(HEMIm^+)_2NTf_2^-$ case (Figure 1d). As such, the OD bands in the $(d_{(2)}\text{-}DEMIm^+)_2NTf_2^-$ spectrum are readily assigned to the same series (A_1, A_2, A_3, and A_4 and free OD) as those observed in the spectrum of the light isotopologue. The $C_{(2)}D$ band near 2350 cm^{-1} appears to be asymmetrically broadened in the $(d_{(2)}\text{-}DEMIm^+)_2NTf_2^-$ spectrum (blue in Figure 2c) with a dominant red-shifted component ($\nu^{bound}_{C_{(2)}D}$) and a weaker higher-energy shoulder. The shoulder appears at the same location as the $C_{(2)}D$ band in the isolated $d_{(2)}$-$DEMIm^+$ cation ($\nu^{free}_{C_{(2)}D}$ in Figure 2a) and that of $d_{(2)}$-$EMIm^+$ (Figure S2a), indicating that only one of the two cations attaches to the anion through the $C_{(2)}H$ group. The $C_{(2)}D$ band in the $(d_{(2)}\text{-}DEMIm^+)_2NTf_2^-$ spectrum (Figure 2c) is broader than that in the $d_{(2)}$-$EMIm^+$ derivative (Figure 2b). In addition, the peak maximum is blue-shifted (by 6 cm^{-1}), with the activity near the $\nu^{free}_{C_{(2)}D}$ feature merging into the overall asymmetrical shape of the band. This shift suggests that the interaction strength of the $C_{(2)}H$ group with the anion is slightly weakened upon incorporation of the hydroxyl group.

To address the role of isomers in the assignments of the spectra, we carried out isomer-selective photochemical hole-burning experiments to establish whether distinct species are present and, if so, to isolate the spectrum of each. This was accomplished using a two-color IR–IR double resonance method described in detail by Yang et al.[53] Briefly, the method

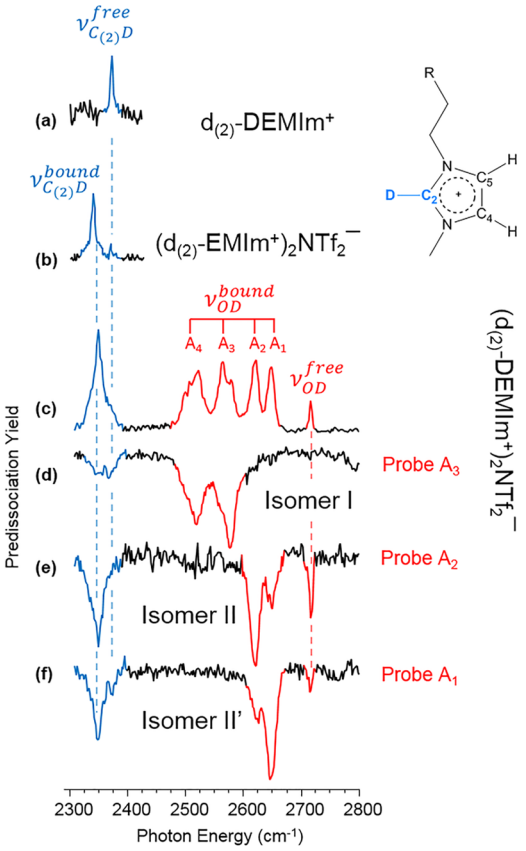

Figure 2. Selectively deuterated N_2-tagged photodissociation spectra of (a) $d_{(2)}$-$DEMIm^+$, (b) $(d_{(2)}\text{-}EMIm^+)_2NTf_2^-$, and (c) $(d_{(2)}\text{-}DEMIm^+)_2NTf_2^-$. Traces (d–f) present IR–IR double resonance spectra of $(d_{(2)}\text{-}DEMIm^+)_2NTf_2^-$ probed at 2578 cm^{-1} (A_3), 2620 cm^{-1} (A_2), and 2645 cm^{-1} (A_1), respectively. R = OD for $d_{(2)}$-$DEMIm^+$ and H for $d_{(2)}$-$EMIm^+$. Measured transition energies are tabulated in Table S1.

relies on the occurrence of features that are unique to each conformer. In such a case, fixing a probe laser on a particular feature monitors the population of that isomer, while a powerful second laser is scanned through the entire spectrum upstream from the probe laser interaction. Because vibrational predissociation is a destructive method for obtaining IR spectra, pump laser excitation of resonances associated with the probed conformer yield a series of dips in the probe signal, thus isolating its spectrum. The method requires an intermediate stage of mass separation between the pump and probe and is thus denoted an IR^2MS^3 class of secondary mass analysis.[38]

The isomer-selective spectra of the $(d_{(2)}\text{-}DEMIm^+)_2NTf_2^-$ isotopologues are reported in Figure 2d–f, which were obtained by probing the A_3, A_2, and A_1 features, respectively. Two isomer classes, denoted I and II, are resolved using double resonance. Additional frequencies were probed that yielded isomer-specific spectra consistent with one of these two classes (Figure S4). Most importantly, the isomer I spectrum (Figure 2d), which accounts for both the A_3 and A_4 OD features, contributes only weakly to the $C_{(2)}D$ region. Most of the $C_{(2)}D$ intensity is thus traced to the type II isomers, which also account for the free OD band as well as the moderately red-shifted A_1 and A_2 OD stretching bands. This behavior establishes that the formation of strong bonds to the OH groups of both cations in isomer I (evidenced by the strongly red-shifted OD stretches) comes at the expense of anionic

DOI: 10.1021/acs.jpclett.8b01130
J. Phys. Chem. Lett. 2018, 9, 2979–2984

bonds to the $C_{(2)}H$ positions on the imidazolium rings. Moreover, the class II isomers display absorptions at the locations of both the free $C_{(2)}D$ ($\nu^{free}_{C_{(2)}D}$) and bound ($\nu^{bound}_{C_{(2)}D}$) regions. As such, the cations in the isomer II class bind to the anion through one $C_{(2)}H$ and one OH group. This information does not, however, resolve the question of whether or not these groups are on the same cation.

The large number of local minima available for the (2,1) clusters that have similar contact modalities does not allow unambiguous structural assignment by comparison with calculated vibrational band patterns, even when simplified by isotopomer-selective spectroscopy. This is especially true given the fact that the simpler binary ion pairs involving [EMIm]-[NTf_2] are analyzed in terms of contributions from several isomers[23,33,34] involving interactions of the $C_{(2)}H$ group with various SO groups on the cis and trans forms of the NTf_2^- scaffold. Attachment of the $C_{(2)}H$ group to the central N atom, the most basic site on the anion (which is protonated in the conjugate $HNTf_2$ acid),[54] has also been identified as a minimum-energy structure in calculations[55] but not invoked in prior experimental studies.[23,33,34] In our survey of calculated structures (six selected structures in Figure S5 with XYZ coordinates in Table S2 and rotatable .pdf structures in Figure S7), we note that all strong $C_{(2)}H$ interactions occur at an SO group on the NTf_2^- anion, with the OH group of the corresponding $HEMIm^+$ cation adopting a nonbonding configuration. This would therefore suggest that one $HEMIm^+$ cation is responsible for both the strongly red-shifted $C_{(2)}D$ feature *and* the free OD feature observed in the spectrum of the ternary complex. As such, the second cation must bind in a different contact motif where the OH group binds to the anion rather than the $C_{(2)}H$ group, accounting for the weak band ($\nu^{free}_{C_{(2)}D}$) in the isomer-selective spectrum (Figure 2f). Many calculated arrangements are consistent with this asymmetrical binding behavior (Figure S5), with a representative structure indicated in Figure 3b. In this geometry, the NTf_2^- is in a trans configuration with the $C_{(2)}H$ of the $HEMIm^+$ (with a free OH) bound to an SO group on the anion, while the OH group on the other cation binds to the oxygen atom on the same sulfur atom. We note that incomplete spectral separation of the two class II isomers leaves open the possibility that isomer II′ actually binds to the anion with both OH groups, leading to two overlapping transitions contributing to peak A_1.

The situation regarding the local interactions in isomer I is more interesting because both cations bind to the anion through their OH groups, raising the possibility that they also interact with each other. The much larger red shifts associated with these OD features (A_3 and A_4 in Figure 2c) relative to those (A_1 and A_2) identified for single OH contacts in isomer II are indeed consistent with cooperative H-bonding to the anion. Harmonic calculations (Figure S3) indicate that such large shifts *require* a cooperative interaction between the two OH groups that acts to enhance the H-bonding interaction with the central N atom on the NTf_2^- anion. The spectral signature of this type of cooperative H-bond to an anion has been reported earlier[51] for methanol attachment to the iodide ion in the $(CH_3OH)_2{\cdot}I^-$ cluster. In that case, two isomers were observed: one in which both OH groups directly bind to the anion and another in which one OH attaches to the oxygen of the second to give an OH···OH···I^- motif. This yields two OH bands split apart by 206 cm^{-1}, with the OH in contact with the ion

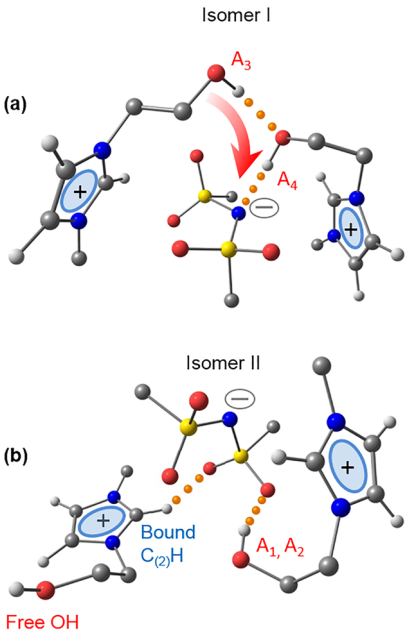

Figure 3. Low-energy structures of $(HEMIm^+)_2NTf_2^-$ calculated at the B3LYP-D3/6-31+G(d) level of theory representing the binding motifs of isomers with (a) and without (b) direct contact between the cations. F atoms of NTf_2^- and aliphatic H atoms of $HEMIm^+$ are omitted for clarity. Labels indicate groups nominally assigned to bands indicated in Figures 1 and 2.

appearing 197 cm^{-1} below that which results from attachment of a single methanol to iodide. The calculated structure consistent with the spectral pattern displayed by isomer I (Figure 3a) indeed displays this type of cooperative arrangement, and its corresponding harmonic band pattern (shown in Figure S3e) recovers both the weak activity in the $C_{(2)}D$ region as well as the two strongly red-shifted bands (A_3 and A_4) in the OD spectral region. These results highlight the importance of the N atom in the interaction with cationic proton donors despite the fact that NTf_2^- is often considered to be dominated by attachment to its SO groups.[23,33,34,56] Support for the role of the N atom as an H-bond acceptor can be found, however, in recent solid-state NMR results on triethylammonium-based protic ILs (PILs),[57] which established that H-bonding from the cation to the central nitrogen atom on NTf_2^- is stronger than that to the oxygen. Calculations also indicate that this binding motif occurs with weakly acidic protons, as illustrated by the structure of the complex formed by attachment of a carboxylic acid-functionalized $EMIm^+$ cation to NTf_2^-, as presented in Figure S6.

Vibrational spectra of the bulk [HEMIm][NTf_2] ionic liquids, with a hydroxyl-functionalized hydrocarbon tail on the cation, have been interpreted in the context of an attractive, H-bonding interaction between the cations. We trace this behavior to the smallest assembly that can display such an effect, the isolated ternary $(HEMIm^+)_2NTf_2^-$ complex, cooled to about 35 K in a photodissociation mass spectrometer. Of the three isomers isolated by double resonance techniques, the one with direct contact between the cations involves a cooperative H-bond in which the OH group on one cation binds to the OH group on the other, which then attaches to the N position at the center of the NTf_2^- anion. This can be formally regarded as an acid−base interaction motif involving cooperativity-enhanced acidity of an OH group interacting with the

DOI: 10.1021/acs.jpclett.8b01130
J. Phys. Chem. Lett. 2018, 9, 2979−2984

protonation site of the NTf_2^- anion. This behavior is thus a microscopic example of a growing class of interactions in hydroxyl-functionalized ionic liquids in which cationic constituents bind together in hydrogen-bonded domains surrounded by anionic counterions.

■ ASSOCIATED CONTENT

Supporting Information

The Supporting Information is available free of charge on the ACS Publications website at DOI: 10.1021/acs.jpclett.8b01130.

Supporting experimental and computational data, as well as rotatable structures (PDF)

■ AUTHOR INFORMATION

Corresponding Authors

*E-mail: mark.johnson@yale.edu (M.A.J.).
*E-mail: ralf.ludwig@uni-rostock.de (R.L.).

ORCID

Fabian S. Menges: 0000-0002-5859-9197
Mark A. Johnson: 0000-0002-1492-6993

Notes

The authors declare no competing financial interest.

■ ACKNOWLEDGMENTS

M.A.J. gratefully acknowledges the U.S. Department of Energy under Grant DE-FG02-06ER15800 for support of the characterization of ionic liquid structure and the Air Force Office of Scientific Research (Grant FA9550-17-1-0267) for the two-color IR−IR capability of the cryogenic ion vibrational spectrometer critical for this study. P.J.K. thanks the National Science Foundation's Center for Aerosol Impacts on Chemistry of the Environment (CAICE) under grant number CHE-1305427 for funding the work on the laser systems critical for these experiments. R.L. gratefully acknowledges financial support from the Deutsche Forschungsgemeinschaft (DFG) under Grant LU 506/14-1. T.N. and A.S. thank the "HERMES-Forschungsförderung" and the "Frauenförderprogramm" of the University of Rostock for supporting their research stays at Yale University. The authors thank Chinh H. Duong and Nan Yang for their help with the double resonance measurements, as well as Profs. E. Castner and M. Maroncelli for their very helpful remarks regarding the presentation of this work.

■ REFERENCES

(1) Castner, E. W.; Margulis, C. J.; Maroncelli, M.; Wishart, J. F. Ionic Liquids: Structure and Photochemical Reactions. *Annu. Rev. Phys. Chem.* **2011**, *62*, 85−105.

(2) Tang, S.; Baker, G. A.; Zhao, H. Ether- and Alcohol-Functionalized Task-Specific Ionic Liquids: Attractive Properties and Applications. *Chem. Soc. Rev.* **2012**, *41* (10), 4030−66.

(3) Vekariya, R. L. A Review of Ionic Liquids: Applications towards Catalytic Organic Transformations. *J. Mol. Liq.* **2017**, *227*, 44−60.

(4) Dorjnamjin, D.; Ariunaa, M.; Shim, Y. K. Synthesis of Silver Nanoparticles using Hydroxyl Functionalized Ionic Liquids and their Antimicrobial Activity. *Int. J. Mol. Sci.* **2008**, *9* (5), 807−819.

(5) Janiak, C. Metal Nanoparticle Synthesis in Ionic Liquids. *Top. Organomet. Chem.* **2013**, *51*, 17−53.

(6) Gao, H. X.; Joo, Y. H.; Twamley, B.; Zhou, Z. Q.; Shreeve, J. M. Hypergolic Ionic Liquids with the 2,2-Dialkyltriazanium Cation. *Angew. Chem., Int. Ed.* **2009**, *48* (15), 2792−2795.

(7) Schneider, S.; Hawkins, T.; Rosander, M.; Vaghjiani, G.; Chambreau, S.; Drake, G. Ionic Liquids as Hypergolic Fuels. *Energy Fuels* **2008**, *22* (4), 2871−2872.

(8) Zhang, Y. Q.; Gao, H. X.; Joo, Y. H.; Shreeve, J. M. Ionic Liquids as Hypergolic Fuels. *Angew. Chem., Int. Ed.* **2011**, *50* (41), 9554−9562.

(9) Hanke, K.; Kaufmann, M.; Schwaab, G.; Havenith, M.; Wolke, C. T.; Gorlova, O.; Johnson, M. A.; Kar, B. P.; Sander, W.; Sanchez-Garcia, E. Understanding the Ionic Liquid $[NC_{4111}][NTf_2]$ from Individual Building Blocks: An IR-Spectroscopic Study. *Phys. Chem. Chem. Phys.* **2015**, *17* (13), 8518−8529.

(10) Wang, Y. T.; Voth, G. A. Unique Spatial Heterogeneity in Ionic Liquids. *J. Am. Chem. Soc.* **2005**, *127* (35), 12192−12193.

(11) Hayes, R.; Warr, G. G.; Atkin, R. Structure and Nanostructure in Ionic Liquids. *Chem. Rev. (Washington, DC, U. S.)* **2015**, *115* (13), 6357−6426.

(12) Triolo, A.; Russina, O.; Bleif, H. J.; Di Cola, E. Nanoscale Segregation in Room Temperature Ionic Liquids. *J. Phys. Chem. B* **2007**, *111* (18), 4641−4644.

(13) Wishart, J. F. Energy Applications of Ionic Liquids. *Energy Environ. Sci.* **2009**, *2* (9), 956−961.

(14) Shkrob, I. A.; Wishart, J. F. Charge Trapping in Imidazolium Ionic Liquids. *J. Phys. Chem. B* **2009**, *113* (16), 5582−5592.

(15) Armand, M.; Endres, F.; MacFarlane, D. R.; Ohno, H.; Scrosati, B. Ionic-Liquid Materials for the Electrochemical Challenges of the Future. *Nat. Mater.* **2009**, *8* (8), 621−629.

(16) Galinski, M.; Lewandowski, A.; Stepniak, I. Ionic Liquids as Electrolytes. *Electrochim. Acta* **2006**, *51* (26), 5567−5580.

(17) Lei, Z. G.; Dai, C. N.; Chen, B. H. Gas Solubility in Ionic Liquids. *Chem. Rev. (Washington, DC, U. S.)* **2014**, *114* (2), 1289−1326.

(18) Hapiot, P.; Lagrost, C. Electrochemical Reactivity in Room-Temperature Ionic Liquids. *Chem. Rev. (Washington, DC, U. S.)* **2008**, *108* (7), 2238−2264.

(19) Weingartner, H.; Cabrele, C.; Herrmann, C. How Ionic Liquids Can Help to Stabilize Native Proteins. *Phys. Chem. Chem. Phys.* **2012**, *14* (2), 415−426.

(20) Rogers, R. D.; Seddon, K. R. Ionic Liquids - Solvents of the Future? *Science* **2003**, *302* (5646), 792−793.

(21) Leal, J. P.; Esperanca, J. M. S. S.; Minas da Piedade, M. E.; Canongia Lopes, J. N.; Rebelo, L. P. N.; Seddon, K. R. The Nature of Ionic Liquids in the Gas Phase. *J. Phys. Chem. A* **2007**, *111* (28), 6176−6182.

(22) Earle, M. J.; Esperanca, J. M. S. S.; Gilea, M. A.; Canongia Lopes, J. N.; Rebelo, L. P. N.; Magee, J. W.; Seddon, K. R.; Widegren, J. A. The Distillation and Volatility of Ionic Liquids. *Nature* **2006**, *439* (7078), 831−834.

(23) Booth, R. S.; Annesley, C. J.; Young, J. W.; Vogelhuber, K. M.; Boatz, J. A.; Stearns, J. A. Identification of Multiple Conformers of the Ionic Liquid $[Emim][Tf_2N]$ in the Gas Phase using IR/UV Action Spectroscopy. *Phys. Chem. Chem. Phys.* **2016**, *18* (25), 17037−17043.

(24) Hunt, P. A.; Ashworth, C. R.; Matthews, R. P. Hydrogen Bonding in Ionic Liquids. *Chem. Soc. Rev.* **2015**, *44* (5), 1257−1288.

(25) Weingartner, H. Understanding Ionic Liquids at the Molecular Level: Facts, Problems, and Controversies. *Angew. Chem., Int. Ed.* **2008**, *47* (4), 654−70.

(26) Knorr, A.; Stange, P.; Fumino, K.; Weinhold, F.; Ludwig, R. Spectroscopic Evidence for Clusters of Like-Charged Ions in Ionic Liquids Stabilized by Cooperative Hydrogen Bonding. *ChemPhysChem* **2016**, *17* (4), 458−462.

(27) Katsyuba, S. A.; Vener, M. V.; Zvereva, E. E.; Fei, Z. F.; Scopelliti, R.; Laurenczy, G.; Yan, N.; Paunescu, E.; Dyson, P. J. How Strong Is Hydrogen Bonding in Ionic Liquids? Combined X-ray Crystallographic, Infrared/Raman Spectroscopic, and Density Functional Theory Study. *J. Phys. Chem. B* **2013**, *117* (30), 9094−9105.

(28) Gorlova, O.; Craig, S. M.; Johnson, M. A. Communication: Spectroscopic Characterization of a Strongly Interacting $C_{(2)}H$ Group on the $EMIM^+$ Cation in the $(EMIM^+)_2X^-$ (X = BF_4, Cl, Br, and I) Ternary Building Blocks of Ionic Liquids. *J. Chem. Phys.* **2017**, *147* (23), 231101.

(29) Tsuzuki, S.; Tokuda, H.; Mikami, M. Theoretical Analysis of the Hydrogen Bond of Imidazolium C_2−H with Anions. *Phys. Chem. Chem. Phys.* **2007**, *9* (34), 4780−4784.

DOI: 10.1021/acs.jpclett.8b01130
J. Phys. Chem. Lett. 2018, 9, 2979−2984

(30) Strate, A.; Niemann, T.; Michalik, D.; Ludwig, R. When Like Charged Ions Attract in Ionic Liquids: Controlling the Formation of Cationic Clusters by the Interaction Strength of the Counterions. *Angew. Chem., Int. Ed.* **2017**, *56* (2), 496−500.
(31) Johnson, C. J.; Fournier, J. A.; Wolke, C. T.; Johnson, M. A. Ionic Liquids from the Bottom Up: Local Assembly Motifs in [EMIM][BF_4] through Cryogenic Ion Spectroscopy. *J. Chem. Phys.* **2013**, *139* (22), 224305.
(32) Fournier, J. A.; Wolke, C. T.; Johnson, C. J.; McCoy, A. B.; Johnson, M. A. Comparison of the Local Binding Motifs in the Imidazolium-Based Ionic Liquids [EMIM][BF_4] and [EMMIM][BF_4] through Cryogenic Ion Vibrational Predissociation Spectroscopy: Unraveling the Roles of Anharmonicity and Intermolecular Interactions. *J. Chem. Phys.* **2015**, *142* (6), 064306.
(33) Cooper, R.; Zolot, A. M.; Boatz, J. A.; Sporleder, D. P.; Stearns, J. A. IR and UV Spectroscopy of Vapor-Phase Jet-Cooled Ionic Liquid [Emim]$^+$[Tf_2N]$^-$: Ion Pair Structure and Photodissociation Dynamics. *J. Phys. Chem. A* **2013**, *117* (47), 12419−12428.
(34) Obi, E. I.; Leavitt, C. M.; Raston, P. L.; Moradi, C. P.; Flynn, S. D.; Vaghjiani, G. L.; Boatz, J. A.; Chambreau, S. D.; Douberly, G. E. Helium Nanodroplet Isolation and Infrared Spectroscopy of the Isolated Ion-Pair 1-Ethyl-3-Methylimidazolium Bis-(trifluoromethylsulfonyl)imide. *J. Phys. Chem. A* **2013**, *117* (37), 9047−9056.
(35) Wolk, A. B.; Leavitt, C. M.; Garand, E.; Johnson, M. A. Cryogenic Ion Chemistry and Spectroscopy. *Acc. Chem. Res.* **2014**, *47* (1), 202−210.
(36) Craig, S. M.; Menges, F. S.; Johnson, M. A. Application of Gas Phase Cryogenic Vibrational Spectroscopy to Characterize the CO_2, CO, N_2 and N_2O Interactions with the Open Coordination Site on a Ni(I) Macrocycle using Dual Cryogenic Ion Traps. *J. Mol. Spectrosc.* **2017**, *332*, 117−123.
(37) Menges, F. S.; Craig, S. M.; Totsch, N.; Bloomfield, A.; Ghosh, S.; Kruger, H. J.; Johnson, M. A. Capture of CO_2 by a Cationic Nickel(I) Complex in the Gas Phase and Characterization of the Bound, Activated CO_2 Molecule by Cryogenic Ion Vibrational Predissociation Spectroscopy. *Angew. Chem., Int. Ed.* **2016**, *55* (4), 1282−1285.
(38) Leavitt, C. M.; Wolk, A. B.; Fournier, J. A.; Kamrath, M. Z.; Garand, E.; Van Stipdonk, M. J.; Johnson, M. A. Isomer-Specific IR-IR Double Resonance Spectroscopy of D_2-Tagged Protonated Dipeptides Prepared in a Cryogenic Ion Trap. *J. Phys. Chem. Lett.* **2012**, *3* (9), 1099−1105.
(39) Grimme, S.; Hansen, A.; Brandenburg, J. G.; Bannwarth, C. Dispersion-Corrected Mean-Field Electronic Structure Methods. *Chem. Rev. (Washington, DC, U. S.)* **2016**, *116* (9), 5105−5154.
(40) Ehrlich, S.; Moellmann, J.; Reckien, W.; Bredow, T.; Grimme, S. System-Dependent Dispersion Coefficients for the DFT-D3 Treatment of Adsorption Processes on Ionic Surfaces. *ChemPhysChem* **2011**, *12* (17), 3414−3420.
(41) Grimme, S.; Bannwarth, C. Ultra-Fast Computation of Electronic Spectra for Large Systems by Tight-Binding Based Simplified Tamm-Dancoff Approximation (sTDA-xTB). *J. Chem. Phys.* **2016**, *145* (5), 054103.
(42) Grimme, S.; Antony, J.; Ehrlich, S.; Krieg, H. A Consistent and Accurate Ab Initio Parametrization of Density Functional Dispersion Correction (DFT-D) for the 94 Elements H-Pu. *J. Chem. Phys.* **2010**, *132* (15), 154104.
(43) Knorr, A.; Ludwig, R. Cation-Cation Clusters in Ionic Liquids: Cooperative Hydrogen Bonding Overcomes Like-Charge Repulsion. *Sci. Rep.* **2015**, DOI: 10.1038/srep17505.
(44) Heimer, N. E.; Del Sesto, R. E.; Meng, Z. Z.; Wilkes, J. S.; Carper, W. R. Vibrational Spectra of Imidazolium Tetrafluoroborate Ionic Liquids. *J. Mol. Liq.* **2006**, *124* (1−3), 84−95.
(45) Roth, C.; Chatzipapadopoulos, S.; Kerle, D.; Friedriszik, F.; Lutgens, M.; Lochbrunner, S.; Kuhn, O.; Ludwig, R. Hydrogen Bonding in Ionic Liquids Probed by Linear and Nonlinear Vibrational Spectroscopy. *New J. Phys.* **2012**, *14*, 105026.
(46) DePalma, J. W.; Kelleher, P. J.; Tavares, L. C.; Johnson, M. A. Coordination-Dependent Spectroscopic Signatures of Divalent Metal Ion Binding to Carboxylate Head Groups: H_2- and He-Tagged Vibrational Spectra of $M^{2+}{\cdot}RCO_2^-$ (M = Mg and Ca, R = -CD_3, -CD_2CD_3) Complexes. *J. Phys. Chem. Lett.* **2017**, *8* (2), 484−488.
(47) Roscioli, J. R.; Diken, E. G.; Johnson, M. A.; Horvath, S.; McCoy, A. B. Prying Apart a Water Molecule with Anionic H-Bonding: A Comparative Spectroscopic Study of the X·H_2O (X = OH, O, F, Cl, and Br) Binary Complexes in the 600−3800 cm^{-1} Region. *J. Phys. Chem. A* **2006**, *110* (15), 4943−4952.
(48) Gorlova, O.; DePalma, J. W.; Wolke, C. T.; Brathwaite, A.; Odbadrakh, T. T.; Jordan, K. D.; McCoy, A. B.; Johnson, M. A. Characterization of the Primary Hydration Shell of the Hydroxide Ion with H_2 Tagging Vibrational Spectroscopy of the $OH^-{\cdot}(H_2O)_{n=2,3}$ and $OD^-{\cdot}(D_2O)_{n=2,3}$ Clusters. *J. Chem. Phys.* **2016**, *145*, 134304.
(49) Robertson, W. H.; Weddle, G. H.; Kelley, J. A.; Johnson, M. A. Solvation of the $Cl^-{\cdot}H_2O$ Complex in CCl_4 Clusters: The Effect of Solvent-Mediated Charge Redistribution on the Ionic H-Bond. *J. Phys. Chem. A* **2002**, *106*, 1205−1209.
(50) Robertson, W. H.; Diken, E. G.; Price, E. A.; Shin, J.-W.; Johnson, M. A. Spectroscopic Determination of the OH^- Solvation Shell in the $OH^-{\cdot}(H_2O)_n$ Clusters. *Science* **2003**, *299*, 1367.
(51) Robertson, W. H.; Karapetian, K.; Ayotte, P.; Jordan, K. D.; Johnson, M. A. Infrared Predissociation Spectroscopy of $I^-{\cdot}(CH_3OH)_n$, n = 1,2: Cooperativity in Asymmetric Solvation. *J. Chem. Phys.* **2002**, *116*, 4853−4857.
(52) Robertson, W. H.; Price, E. A.; Weber, J. M.; Shin, J.-W.; Weddle, G. H.; Johnson, M. A. Infrared Signatures of a Water Molecule Attached to Triatomic Domains of Molecular Anions: Evolution of the H-bonding Configuration with Domain Length. *J. Phys. Chem. A* **2003**, *107*, 6527−6532.
(53) Yang, N.; Duong, C. H.; Kelleher, P. J.; Johnson, M. A.; McCoy, A. B. Isolation of Site-Specific Anharmonicities of Individual Water Molecules in the $I^-{\cdot}(H_2O)_2$ Complex using Tag-Free, Isotopomer Selective IR-IR Double Resonance. *Chem. Phys. Lett.* **2017**, *690*, 159−171.
(54) Akai, N.; Parazs, D.; Kawai, A.; Shibuya, K. Cryogenic Neon Matrix-isolation FTIR Spectroscopy of Evaporated Ionic Liquids: Geometrical Structure of Cation-Anion 1:1 Pair in the Gas Phase. *J. Phys. Chem. B* **2009**, *113* (14), 4756−4762.
(55) Zhang, S. G.; Qi, X. J.; Ma, X. Y.; Lu, L. J.; Zhang, Q. H.; Deng, Y. Q. Investigation of Cation-Anion Interaction in 1-(2-Hydroxyethyl)-3-Methylimidazolium-Based Ion Pairs by Density Functional Theory Calculations and Experiments. *J. Phys. Org. Chem.* **2012**, *25* (3), 248−257.
(56) Lall-Ramnarine, S. I.; Zhao, M.; Rodriguez, C.; Fernandez, R.; Zmich, N.; Fernandez, E. D.; Dhiman, S. B.; Castner, E. W.; Wishart, J. F. Connecting Structural and Transport Properties of Ionic Liquids with Cationic Oligoether Chains. *J. Electrochem. Soc.* **2017**, *164* (8), H5247−H5262.
(57) Khudozhitkov, A. E.; Stange, P.; Golub, B.; Paschek, D.; Stepanov, A. G.; Kolokolov, D. I.; Ludwig, R. Characterization of Doubly Ionic Hydrogen Bonds in Protic Ionic Liquids by NMR Deuteron Quadrupole Coupling Constants: Differences to H-bonds in Amides, Peptides, and Proteins. *Angew. Chem., Int. Ed.* **2017**, *56* (45), 14310−14314.
(58) Plyler, E. K. Infrared Spectra of Methanol, Ethanol, and Normal-Propanol. *J. Res. Natl. Bur. Stand. (U. S.)* **1952**, *48* (4), 281−286.

DOI: 10.1021/acs.jpclett.8b01130
J. Phys. Chem. Lett. 2018, 9, 2979−2984